Electronic Supplementary Material (ESI) for Chemical Communications

Supporting Information

Molecular Engineering of Excitation Energy Hopping in Self-assembled Porphyrin Boxes

Hee Won Bahng, [a] Pyosang Kim,[a] Young Mo Sung, [a] Chihiro Maeda,*[,b] Atsuhiro Osuka,*[,c] and Dongho Kim*[,a]

[a] Department of Chemistry, Yonsei University, Seoul 120-749, Korea, [b]Keio University, Kohoku-ku, Yokohama 223-8522, Japan., Department of Chemistry, Graduate School of Science, Kyoto University, Sakyo-ku, Kyoto, 606-8502, Japan, [c] Department of Applied Chemistry, Faculty of Science and Technology

E-mail: dongho@yonsei.ac.kr, osuka@kuchem.kyoto-u.ac.jp, cmaeda@applc.keio.ac.jp

Contents

1. Experimental Details

Instrumentation and Materials

^{1}H NMR spectra were taken on a JEOL ECA-600 spectrometer, and chemical shifts were reported as the delta scale in ppm as internal reference (δ= 7.260 for ^{1}H NMR, for $CDCl_3$; δ = 8.700 for ^{1}H NMR, for pyridine-d_5, and δ = 149.5 for ^{13}C NMR, for pyridine-d_5). Mass spectra were recorded on a Shimadzu/KRATOS KOMPACT MALDI 4 spectrometer, using positive-MALDI ionization method with dithranol matrix. Analytical GPC-HPLC was performed on JAIGEL 2.5H-AF, 3H-AF, and 4H-AF columns (eluent, $CHCl_3$; flow rate, 1.2 mL/min) in series with JASCO HPLC system using multiwavelength detector MD-915. Unless otherwise noted, materials obtained from commercial suppliers were used without further purification. Dry Et_3N, *i*-Pr_2NH and MeOH were distilled from CaH_2.

Steady-State Spectroscopy. The sample solutions were prepared in approximately micromolar concentrations in toluene. Toluene was purchased from Sigma-Aldrich (spectrophotometric grade). Absorption spectra were obtained by using a UV-vis spectrometer (Cary5000, Varian), and fluorescence spectra were obtained by using a fluorometer (F-2500, Hitachi). The fluorescence quantum yields were obtained using rhodamine 6G in methanol as reference ($_f$ = 0.95), with $_{ex}$ = 480nm.

Time-Resolved Fluorescence Decay and Anisotropy. A time-correlated single-photon-counting (TCSPC) system was used for measurements of spontaneous fluorescence decay and fluorescence anisotropy decay. As an excitation light source, we used a mode-locked Ti:sapphire laser (MaiTai BB, Spectra Physics) which provides ultrashort pulse (80 fs at full width half maximum, fwhm) with high repetition rate (80 MHz). This high repetition rate

slows down to 1M ~ 800 kHz by using homemade pulse-picker. The pulse-picked output pulse was frequency-doubled by a 1 mm thickness of a BBO crystal (EKSMA). The fluorescence was collected by a microchannel plate photomultiplier (MCP-PMT, R3809U-51, Hamamatsu) with a thermoelectric cooler (C4878, Hamamatsu) connected to a TCSPC board (SPC-130, Becker & Hickel GmbH). The overall instrumental response function was about 25 ps (fwhm). A vertically polarized pump pulse by a Glan-laser polarizer was irradiated to samples, and a sheet polarizer, set at an angle complementary to the magic angle (54.7°), was placed in the fluorescence collection path to obtain polarization-independent fluorescence decays. Time-resolved fluorescence anisotropy decays were obtained by changing the detection polarization on the fluorescence path to parallel or perpendicular to the polarization of the excitation pulses. The calculation of anisotropy decay then was followed by

$$r(t) = \frac{I_{VV}(t) - GI_{VH}(t)}{I_{VV}(t) + 2GI_{VH}(t)}$$

Where $I_{VV}(t)$ [or $I_{VH}(t)$] is the fluorescence decay when the excitation light is vertically polarized and only the vertical (or horizontally) polarized portion of fluorescence is detected, and the first and second subscripts represent excitation and detection polarization, respectively. The factor G is defined by $I_{HV}(t)/I_{HH}(t)$, which is equal to the ration of the sensitivities of the detection system for vertical and horizontal polarization.

Femtosecond Transient Absorption Measurements. The femtosecond time-resolved transient absorption (TA) spectrometer consisted of homemade noncollinear optical parametric amplifier (NOPA) pumped by a Ti:sapphire regenerative amplifier system (Integra-C,

Quantronix) operating at 1 kHz repetition rate and an optical detection system. The generated visible NOPA pulses had a pulse width of ~ 100 fs and an average power of 1 mW in the range 480-700 nm which were used as pump pulses. White light continuum (WLC) probe pulses were generated using a sapphire window (3 mm of thickness) by focusing of small portion of the fundamental 800 nm pulses which was picked off by a quartz plate before entering to the NOPA. The time delay between pump and probe beams was carefully controlled by making the pump beam travel along a variable optical delay (ILS250, Newport). Intensities of the spectrally dispersed WLC probe pulses are monitored by miniature spectrograph (USB2000+, OceanOptics). To obtain the time-resolved transient absorption difference signal (ΔA) at a specific time, the pump pulses were chopped at 25 Hz and absorption spectra intensities were saved alternately with or without pump pulse. Typically, 6000 pulses excite samples to obtain the TA spectra at a particular delay time. The polarization angle between pump and probe beam was set at the magic angle (54.7°) using a Glan-laser polarizer with a half-wave retarder in order to prevent polarization-dependent signals. Cross-correlation fwhm in pump-probe experiments was less than 200 fs and chirp of WLC probe pulses was measured to be 800 fs in the 400-800 nm region. To minimize chirp, all reflection optics in probe beam path and 2 mm path length of quartz cell were used. After fluorescence and TA experiments, we carefully checked absorption spectra of all compounds to avoid artifact from degradation and photo-oxidation of samples. The HPLC grade solvents were used in all steady-state and time-resolved spectroscopic studies. The three-dimensional data sets of A versus time and wavelength were subjected to singular value decomposition and global fitting to obtain the

kinetic time constants and their associated spectra using Surface Xplorer software (Ultrafast Systems).

Femtosecond Transient Absorption Anisotropy Decay. A dual-beam femtosecond time-resolved transient absorption (TA) spectrometer consisted of two independently tunable homemade optical parametric amplifiers (OPA) pumped by a regeneratively amplified Ti:sapphire laser system (Hurricane-X, Spectra-Physics) operating at 3 kHz repetition rate and an optical detection system. The OPA was based on noncollinearly phase-matching geometry, which was easily color-tuned by controlling optical delay between white light continuum seed pulses (450-1400 nm) and visible pump pulses (400 nm) produced by using a sapphire window and BBO crystal, respectively. The generated visible OPA pulses had a pulse width of ~35 fs and an average power of 10 mW at 5 kHz repetition rate in the range of 500-700 nm after a fused-silica prism compressor. Two OPA pulses were used as the pump and probe pulses, respectively, for TA measurements. The probe beam was split into two parts. The one part of the probe beam was overlapped with the pump beam at the sample to monitor the transient (signal), while the other part of the probe beam was passed through the sample without overlapping the pump beam to compensate the intensity fluctuation of probe beam. The time delay between pump and probe beams was carefully controlled by making the pump beam travel along a variable optical delay (ILS250, Newport). To obtain the time-resolved transient absorption difference signal at specific wavelength, the monitoring wavelength was selected by using a narrow interface filter (fwhm ~ 10nm). By chopping the pump pulses at 1.5 kHz, the modulated probe pulses as well as the reference pulses were detected by two separated photodiodes (Femtowatt Photoreceiver, New Focus). The modulated signals of the probe

pulses were measured by a gated integrator (SR250, SRS) and a lock-in amplifier (DSP7265, EG&G) and stored in a personal computer for further signal processing. In general experimental conditions, time resolutions of less than 50 fs were achieved. For time-resolved transient absorption anisotropy (TAA) measurement, both $I_{\parallel}$ and $I_{\perp}$ signals were collected simultaneously by combination of polarizing beam splitter cube and dual lock-in amplifiers as the following equation:

$$r(t) = \frac{I_{\parallel} - I_{\perp}}{I_{\parallel} + 2I_{\perp}}$$

where $I_{\parallel}$ and $I_{\perp}$ represent TA singnals with the polarization of the pump and probe pulses being mutually parallel and perpendicular, respectively. The pump pulses were set to vertical polarization and that of probe pulse was set to 45° with respect to the pump pulse by using Glan-laser polarizers and half-wave plates. After the probe pulse passes through the sample cell, it was split by a polarizing beam splitter cube and then detected by two separated photodiodes. Two gated integrators and two lock-in amplifiers record the signal simultaneously within a single scan. As a standard, anisotropy measurement showed a clean single-exponential decay with reorientational relaxation time of 120 ps and the initial anisotropy value r(0) of 0.39 for rhodamine 6G dye in methanol, which are well-matched in other reference. For all TAA measurements, the wavelength of the pump and probe pulse was set to 530 and 580 nm with an average power of less than 40 μW and a thin absorption cell with a path length of 1mm was used to eliminate additional chirping.

2. Supporting Information

(1) Synthesis of D2 and D3

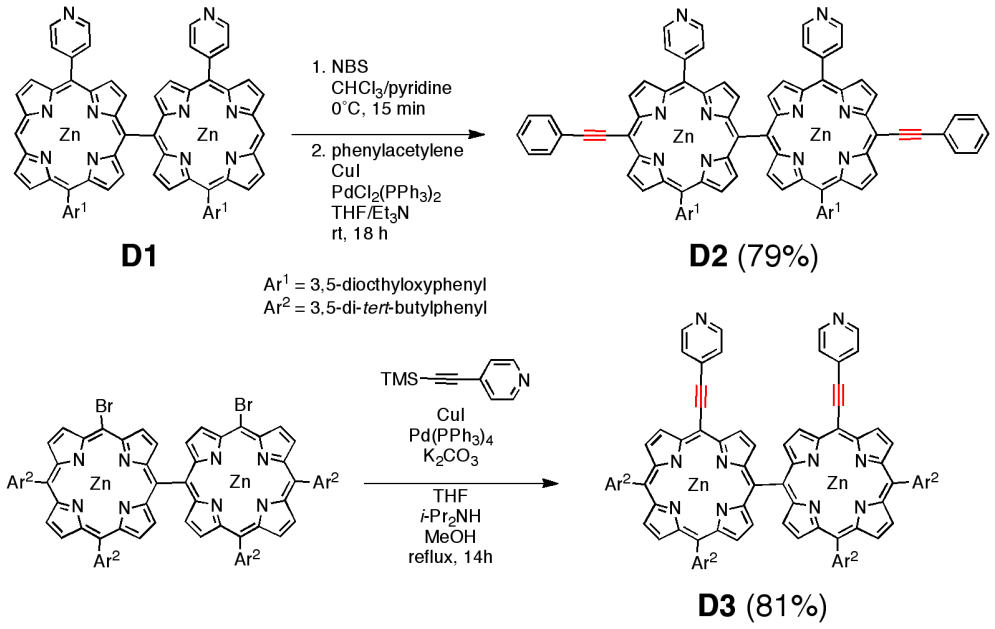

Scheme S1. Synthesis of **D2** and **D3**

Synthetic routs to **D2** and **D3** were shown in Scheme S1. Bromination of **D1** with NBS and subsequent Sonogashira coupling reaction with phenylacetylene provided **D2** in 79% yield. **D3** was prepared via Sonogashira reaction of 10,10′-dibromo-*meso*-*meso*-linked diporphyrin with 4-trimethylsilylethynylpyridine through in situ trimethylsilyl group deprotection in 81% yield.

Synthesis of D2

N-Bromosuccinimide (7.86 mg, 44.2 μmol) was added to a $CHCl_3$/pyridine (10 mL/1 drop) solution of compound **D1** (32.3 mg, 20.6 μmol) at 0 °C, and the resulting mixture was stirred for 15 min before the reaction was quenched with acetone. Organic solvents were evaporated to dryness. A flask containing the residue, CuI (0.53 mg, 2.8 μmol), and $PdCl_2(PPh_3)_2$ (1.47 mg, 2.09 μmol) was purged with N_2, and then charged with anhydrous THF (4 mL) and dry Et_3N (1 mL). After this solution was frozen with liquid nitrogen, phenylacetylene (0.060 mL. 540 μmol) was added and the mixture was then degassed. The mixture was stirred for 18 h at

room temperature, quenched with water, and evaporated to remove organic solvents. The residue was separated over a silica gel column with $CHCl_3$ to give the compound **D2** (28.6 mg, 16.2 μmol, 79%).

^{1}H NMR ($CDCl_3$) δ 9.87 (d, J = 4.1 Hz, 2H, β), 9.58 (d, J = 4.1 Hz, 2H, β), 9.11 (d, J = 4.1 Hz, 2H, β), 8.51 (d, J = 4.1 Hz, 2H, β), 8.09 (d, J = 6,4 Hz, 4H, *o*-Ph), 7.76 (d, J = 4.1 Hz, 2H, β), 7.61 (d, J = 4.1 Hz, 2H, β), 7,65 (t, J = 6.7 Hz, 4H, *m*-Ph), 7.58 (t, J = 7.6 Hz, 2H, *p*-Ph), 7.54 (d, J = 4.1 Hz, 2H, β), 7.32 (d, J = 4.1 Hz, 2H, β), 7.27 (s, 2H, Ar), 7.26 (s, 2H, Ar), 6.68 (s, 2H, Ar), 6.65 (d, J = 6.4 Hz, 2H, Py), 6.42 (d, J = 6.0 Hz, 2H, Py), 3.96 (t, J = 6.4 Hz, 4H, OCH_2), 3.89 (br, 4H, OCH_2), 3.10 (d, J = 5.9 Hz, 2H, Py), 2.60 (d, J = 5.4 Hz, 2H, Py), 1.71 (m, 4H, CH_2), 1.35 (m, 4H, CH_2), 1.28-0.91 (40H, CH_2), 0.74 (t, J = 6.6 Hz, 6H, CH_3), 0.56 (t, J = 6.7 Hz, 6H, CH_3); ^{1}H NMR (pyridine-d_5) δ 10.23 (d, J = 4.6 Hz, 2H, β), 9.85 (d, J = 4.6 Hz, 2H, β), 9.53 (d, J = 4.6 Hz, 2H, β), 9.32 (d, J = 4.6 Hz, 2H, β), 9.28 (d, J = 4.6 Hz, 2H, β), 9.00 (d, J = 4.1 Hz, 2H, β), 8.83 (d, J = 5.5 Hz, 4H, Py), 8.57 (s, 2H, Ar), 8.56 (s, 2H, Ar), 8.49 (d, J = 4.6 Hz, 2H, β), 8.48 (s, 2H, Ar), 8.46 (s, 2H, Ar), 8.26 (d, J = 4.6 Hz, 2H, β), 8.15 (s, 2H, Ar), 7.99 (s, 2H, Ar), 7.88 (d, J = 6.0 Hz, 2H, Py), 1.64 (s, 18H, *t*-Bu), 1.63 (s, 18H, *t*-Bu), 1.49 (s, 18H, *t*-Bu), 1.48 (s, 18H, *t*-Bu); ^{13}C NMR (pyridine-d_5) δ 158.91, 155.46, 155.18, 153.04, 152.81, 151.04, 150.83, 150.49, 149.33, 148.52, 145.08, 134.73, 134.45, 133.47, 132.48, 132.31, 132.00, 131.82, 131.47, 131.39, 129.72, 129.29, 128.94, 124.63, 123.97, 122.06, 119.94, 114.97, 114.91, 101.47, 100.71, 97.06, 94.03, 68.46, 31.84, 31.87, 29.63, 29.60, 29.51, 29.49, 29.37, 26.30, 26.28, 22.76, 14.11; MALDI-TOF-MS: m/z = 1762; calcd for $C_{110}H_{108}N_{10}O_4Zn_2$ = 1765.

Synthesis of D3

To a dry THF (8 mL) solution of 10,10′-dibromo-15,15′,20,20′-tetrakis(3,5-di-*tert*-butylphenyl)-5,5′-*meso*-*meso*-linked zinc(II)-diporphyrin (62.7 mg, 37.3 μmol), 4-trimethylsilylethynylpyridine (67.0 mg, 383 μmol), CuI (1.07 mg, 5.63 μmol), $Pd(PPh_3)_4$ (18.3 mg, 15.8 μmol), and K_2CO_3 (24.8 mg, 180 μmol) was added dry *i*-PrNH (1.0 mL), dry MeOH (1.0 mL) and the resulting solution was degassed. The mixture was stirred for 14 h at 70 °C. After the organic solvents were evaporated, the residue was dissolved in $CHCl_3$ and demetallation with conc. HCl. The mixture was then washed with $NaHCO_3$aq and evaporated. The residue was separated over a silica gel column (eluent: $CHCl_3$, then $CHCl_3$/EtOH = 99/1) to

give the corresponding free base diporphyrin, which was converted into desired product via zinc(II) insertion with excess $Zn(OAc)_2$ and recrystallization with $CHCl_3/CH_3CN$ (51.6 mg, 30.3 μmol, 81%).

^{1}H NMR ($CDCl_3$ with $BuNH_2$ (25 eq vs **3**)) δ 9.14 (d, J = 4.1 Hz, 2H, β), 9.00 (d, J = 4.1 Hz, 2H, β), 8.88, (d, J = 4.1 Hz, 2H, β), 8.87 (d, J = 4.1 Hz, 2H, β), 8.81 (d, J = 4.1 Hz, 2H, β), 8.38 (d, J = 4.1 Hz, 2H, β), 8.25 (s, 2H, Ar), 8.03 (d, J = 4.1 Hz, 2H, β), 7.94 (s, 2H, Ar), 7.87 (2H+2H, Ar), 7.84 (s, 2H, Ar), 7.73 (d, J = 4.1 Hz, 2H, β), 7.55 (s, 2H, Ar), 6.44 (d, J = 6.4 Hz, 4H, Py), 3.13 (d, J = 6.0 Hz, 4H, Py), 1.68 (s, 18H, *t*-Bu), 1.51 (s, 18H, *t*-Bu), 1.32 (s, 18H, *t*-Bu), 1.29 (s, 18H, *t*-Bu); ^{1}H NMR (pyridine-d_5) δ 9.14 (d, J = 4.1 Hz, 2H, β), 9.00 (d, J = 4.1 Hz, 2H, β), 8.88, (d, J = 4.1 Hz, 2H, β), 8.87 (d, J = 4.1 Hz, 2H, β), 8.81 (d, J = 4.1 Hz, 2H, β), 8.38 (d, J = 4.1 Hz, 2H, β), 8.25 (s, 2H, Ar), 8.03 (d, J = 4.1 Hz, 2H, β), 7.94 (s, 2H, Ar), 7.87 (2H+2H, Ar), 7.84 (s, 2H, Ar), 7.73 (d, J = 4.1 Hz, 2H, β), 7.55 (s, 2H, Ar), 6.44 (d, J = 6.4 Hz, 4H, Py), 3.13 (d, J = 6.0 Hz, 4H, Py), 1.68 (s, 18H, *t*-Bu), 1.51 (s, 18H, *t*-Bu), 1.32 (s, 18H, *t*-Bu), 1.29 (s, 18H, *t*-Bu); ^{13}C NMR (pyridine-d_5) δ 156.03, 155.02, 153.54, 152.83, 151.70, 151.37, 150.69, 150.54, 149.43, 149.14, 142.70, 142.67, 134.10, 133.01, 132.75, 132.24, 130.99, 130.89, 130.66, 130.19, 130.11, 126.63, 125.46, 125.13, 121.48, 121.34, 121.25, 98.75, 98.36, 94.12, 35.24, 35.08, 31.75, 31.62; MALDI-TOF-MS: m/z = 1699; calcd for $C_{110}H_{108}N_{10}Zn_2$ = 1701.

(2) Excitonic Coupling in *meso-meso* Linked Porphyrin Dimer and Porphyrin Box.

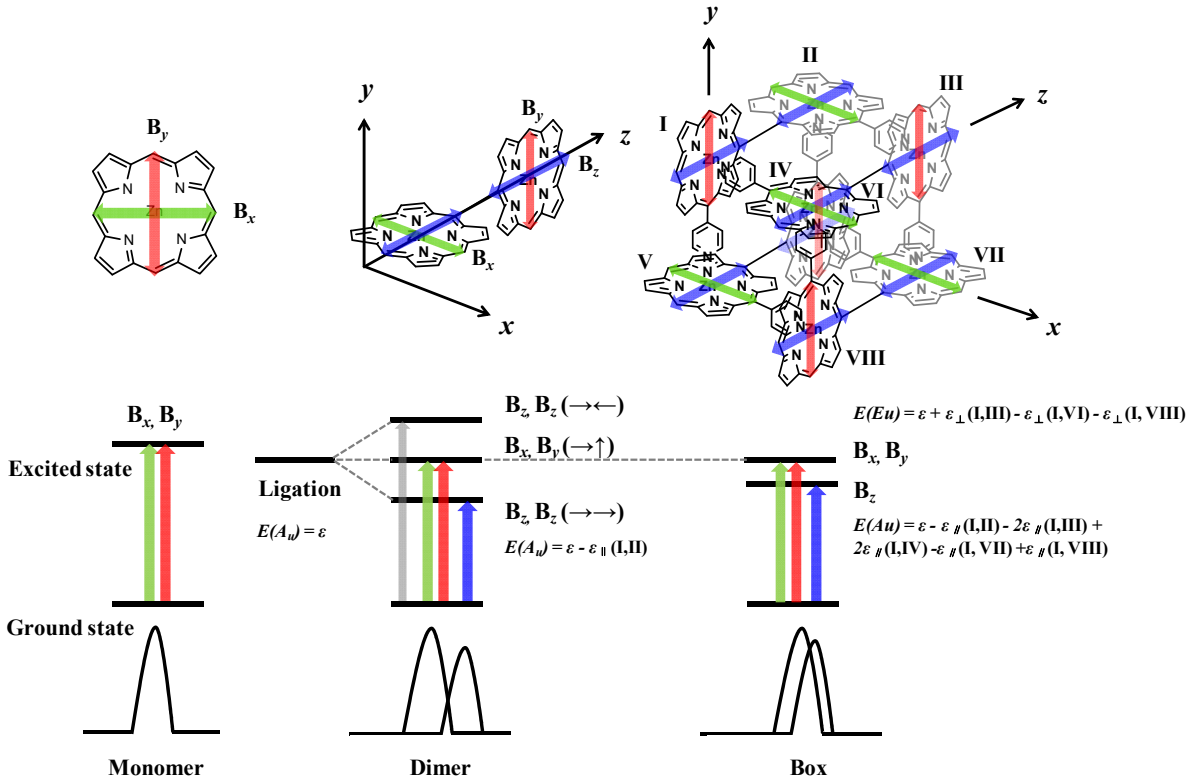

Scheme S2. Exciton Coupling in the Monomer, *meso-meso* Linked Diporphyrin, and Porphyrin Box

Similar to other free *meso-meso*-linked zinc(II) diporphyrins, **D*n*** display the split Soret bands due to exciton coupling. The Soret band of zinc(II) porphyrin monomer has two perpendicular transition dipole moments, **B*x*** and **B*y***, that are degenerate in a simple monomer. In a *meso-meso*-linked zinc-(II) diporphyrin, however, parallel **B*z*** dipole moments couple effectively, whereas the other dipole interactions should be virtually zero because of an averaged perpendicular conformation. Thus, the Soret bands of **D*n*** are split into a red-shifted **B*z*** component and unperturbed **B*x*** and **B*y*** components. It is known that the dihedral angle is not strictly fixed as 90º but has a distribution of 90 ± 20º.[9] This has been taken as a cause of the broad Soret band of *meso-meso* linked zinc(II) diporphyrins. The electronic interaction should be minimum at exactly 90º and increases with a decrease in the dihedral angle. This was indeed confirmed by the examination of a series of permanently distorted 1, -

dioxylmethylene-strapped *meso-meso*-linked zinc(II) diporphyrins with dihedral angles of less than 90º and was used as a switching excitation energy-transfer component. In this context, it is interesting to note that the porphyrin boxes **B*n*** exhibit common features of a small Soret band splitting and fluorescence spectrum with distinct vibrational structures, indicating an attenuation of the electronic interactions within a *meso-meso*-linked zinc(II) diporphyrin in comparison to those in normal *meso-meso*-linked zinc(II) diporphyrins. We interpreted this attenuation in terms of the rigidification of a strictly perpendicular conformation of *meso-meso*-linked zinc(II) diporphyrin as a result of simultaneous multipoint coordinative interactions.

To explain the origin of the Soret band of **B*n***, the excitonic dipole coupling scheme is introduced. The Soret band splitting in the *meso-meso*-linked zinc(II) diporphyrin could be explained by simple excitonic dipole coupling between zinc(II) porphyrin monomers. In the case of **B*n***, however, more complicated Soret band splittings are expected, because various dipole-dipole excitonic interactions are possible among eight mutually perpendicular porphyrin units. Among sixteen possible exciton coupling states of **B*n***, only two states are transition-allowed. The low-energy Soret state indicates excitonic dipole-dipole interactions among eight parallel transition dipole moments along the *z*-axis (blue arrows), whereas the high-energy Soret state implies excitonic dipole-dipole interactions among four parallel transition dipole moments along the *x*- or *y*-axis (red or green arrows). The blue shift in the low-energy Soret band of **B*n*** is due to H-type dipole coupling between molecule I and molecules IV, V, and VIII.

The geometry of **B*n*** has C_{4h} symmetry,and the sixteen possible exciton coupling states with k = 0, ±1, ±2, ±3, 4; u = //, ⊥ span the irreducible representations of the C_{4h} group, where u = // or ⊥

represents parallel or perpendicular orientation to the fourfold axis of **B*n*** (the z-axis). Of these possible states, only state $|0, /\!/\rangle(Au)$ and twofold degenerate state $|\pm1, \perp\rangle(Eu)$ are connected by dipole-allowed transitions. The $|0, /\!/\rangle(Au)$ state implies excitonic dipole-dipole interaction between eight parallel transition dipole moments along the z-axis (blue arrows in Scheme S1, right), whereas the twofold degenerate state $|\pm1, \perp\rangle(Eu)$ indicates excitonic dipole-dipole interaction among four parallel transition dipole moments along the x- or y-axis (red or green arrows). The energies of these two states are given as

$E(Au) = - \ _{/\!/}(\mathrm{I,II}) - 2\ _{/\!/}(\mathrm{I,III}) + 2\ _{/\!/}(\mathrm{I,IV}) - \ _{/\!/}(\mathrm{I, VII}) + \ _{/\!/}(\mathrm{I, VIII})$

$E(Eu) = + \ _{\perp}(\mathrm{I,III}) - \ _{\perp}(\mathrm{I,VI}) - \ _{\perp}(\mathrm{I, VIII})$

where is the energy of the locally excited-state plus the energy change of the constituents in aggregate, and the coupling energy between the transition dipoles e.g. $_{/\!/}(\mathrm{I,II}) = \langle \mathrm{I}, /\!/ | V | \mathrm{II}, /\!/ \rangle$ and $_{\perp}(\mathrm{I,III}) = \langle \mathrm{I}, \perp | V | \mathrm{III}, \perp \rangle$, where V is the intermolecular perturbation potential e.g.

$$V_{AB} = \frac{|\mu_A \mu_B|}{4\pi\Xi_0 R^3}(2\cos\theta_A \cos\theta_B + \sin\theta_A \sin\theta_B \cos\varphi)$$

The angles define the relative orientations of the transition dipole moments in molecules A and B.

(3) TAA Masurements and Excitation Energy Hopping Time in Multichromophoric Systems

The observed TAA decays are strongly associated with the excitation energy transfer (EET) in the regime of Förster-type incoherent energy hopping process. In multichromophoric arrays,

the EET is followed by the reorientation of transition dipole, which leads to fast depolarization in the TAA decay, however, the anisotropy depolarization time does not represent the EET time directly, because both kinetics do not occur on a single donor-acceptor pair. An appropriate theoretical model is needed to calculate the EET time from the TAA measurements. By using the polygon model, we could derive the excitation energy hopping (EEH) time from the TAA measurements. Previously, Fleming and coworkers[S1] proposed a structural model involving circular arrangements of pigments, in which the transition dipoles of pigments are organized on a circle and their orientations are uniformly distributed within the 2-dimensional ring plane.

Regular Polygon Model

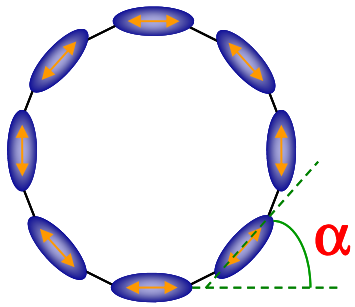

Assumption

All N sites are equivalent and only the nearest neighbor hopping is considered

N : the effective number of chromophores (hopping sites)
α : the angle between adjacent transition dipole moments

Assuming a random walk formalism of anisotropy decay, this model yields numerical relationships between the EET time and the analytical depolarization which is illustrated by

$$\tau_{depolarization} = \frac{\tau_{hopping}}{4(1-\cos^2(2\pi/N))} = \frac{\tau_{hopping}}{4(1-\cos^2\alpha)} \quad \text{(S1)}$$

where α is the angle between adjacent transition dipoles and equals to $360°/N$ if all N sites are equivalent and only the nearest neighbor hopping is considered. $\tau_{hopping}$ is the inverse of the nearest neighbor hopping rate. Eq (S1) is understood by considering that the depolarization is complete when the transition dipole migrates through 90° and that how many hops are

required for this rotation to be accomplished. Based on the polygon model, it is hard to derive EET times from TAA decay components in **B*n*** whose transition dipole moments participating in EET are described as 3-dimensional structure. So the angle between the adjacent transition dipole moments, α could not be defined. Nevertheless, considering the similar tendencies observed in the pump-power dependent TA and TAA decays (Figure 3 and Figure S2) in **B*n***, we could understand that the solvent affect the EET times of **B*n*.**

Acknowledgements

The work at Yonsei was supported by WCU (World Class University) programs (R32-2010-10217-0) and an AFSOR/APARD grant (no. FA2386-09-1-4092). The work at Kyoto was supported by Grants-in-Aid for Scientific Research (nos. 22245006 and 20108001).

References

(S1) S. E. Bradforth, R. Jimenez, F. van Mourik, R. van Grondelle, G. R. Fleming, *J. Phys. Chem.* 1995, **99**, 16179.

Table S1. Calculated molecular weights and GPC-HPLC retention times

Compound	Molecular Formula	Mcalcd	Time (min)
B1	$C_{376}H_{400}N_{40}O_{16}Zn_8$	6260	21.4
B2	$C_{440}H_{432}N_{40}O_{16}Zn_8$	7060	21.2
B3	$C_{440}H_{432}N_{40}Zn_8$	6808	21.6
Ref	$C_{128}H_{166}N_8O_8Zn_2$	2076	23.1

Table S2. Band Maxima of Absorption and Fluoresence Spectra of **D*n*** and **B*n***[a]

[a] The band position was determined by the Gaussian band-fitting process. [b] Φ_f indicates the fluorescence quantum yield measured by excitation at high energy Soret bands.

		Absorption					Fluorescence		
Sample	Solvent	Soret (high) (nm)	Soret (low) (nm)	ΔE_{soret} (cm^{-1})	Q(1,0) (nm)	Q(0,0) (nm)	Q(0,0) (nm)	Q(0.1) (nm)	Φ_f[b]
D1	pyridine	424	459	1978	568	607	631	666	0.08
D2	pyridine	447	482	1624	590	642	-	670	0.22
D3	pyridine	449	486	1696	595	641	685	716	0.14
B1	CH_2Cl_2	426	444	952	566	600	617	670	0.04
B2	CH_2Cl_2	451	470	896	590	630	645	706	0.07
B3	CH_2Cl_2	454	476	1018	594	641	657	711	0.07

Table S3. Fitted Fluorescence Lifetimes and Anisotropy Decay Parameters of **D*n*** and **B*n***[a]

[a] An excitation wavelength of 420 nm and 450 nm were applied to **D1**/**B1** and **D2**/**B2**, **D3**/**B3** experiments. [b] Using the relation $I(t) = A_1 \exp(-t/\ )$, where $I(t)$ is the time-dependent fluorescence intensity, A the amplitude, and the fitted fluorescence lifetime. [c] Using the relation $r(t) = r_0 \exp(-t/\ _{rot})$, where $r(t)$ is the time-dependent fluorescence anisotropy $\{r(t) = [I_{\parallel}(t)-GI_{\perp}(t)] / [I_{\parallel}(t)+2GI_{\perp}(t)]\}$, r_0 the initial anisotropy value, and $_{rot}$ the fitted rotational decay or rise time.

Sample	Solvent	Fluorescence lifetime τ[b] (ns)	Anisotropy decay parameters[c]	
			r_0	τ_{rot} (ns)
D1	pyridine	1.6	-0.05	0.8
D2	pyridine	1.3	-0.07	1.2
D3	pyridine	1.5	0.03	0.4
B1	CH_2Cl_2	1.7	0.01	2.5
B2	CH_2Cl_2	1.5	-0.02	4.9
B3	CH_2Cl_2	1.3	0.01	2.6

Table S4. Transient Absorption Decay Parameters for **B*n*** Depending on the Pump Power[a]

[a] The pump and probe wavelengths are 570nm and 520nm, respectively. [b] Using the relation $\Delta OD(t) = A_1 \exp(-t/\tau_1) + A_2 \exp(-t/\tau_2) + A_3 \exp(-t/\tau_3)$, where $\Delta OD(t)$ is the transient absorption intensity, A the amplitude (noted in paretheses as the normalizes percentage, i.e.,$[A_i/(A_1+A_2+A_3)] \times 100$), and the fitted decay time.

Pump Power (mW)	Fitted decay times (ps)[b]			
	Dichloromethane		Toluene	
	τ_1 and τ_2	τ_3	τ_1 and τ_2	τ_3
			B1	
4.0	2, 18 (59%)	1400 (41%)	2.0, 11 (86%)	1400 (14%)
2.0	2, 18 (46%)	1400 (54%)	2.0, 11 (78%)	1400 (22%)
1.0	2, 18 (33%)	1400 (67%)	2.0, 11 (38%)	1400 (62%)
0.5	2, 18 (24%)	1400 (76%)	2.0, 11 (26%)	1400 (74%)
			B2	
4.0	1.3, 17 (59%)	1400 (41%)	0.4, 3.4 (87%)	1400 (13%)
2.0	1.3, 17 (48%)	1400 (52%)	0.4, 3.4 (81%)	1400 (19%)
1.0	1.3, 17 (40%)	1400 (60%)	0.4, 3.4 (40%)	1400 (60%)
0.5	1.3, 17 (26%)	1400 (74%)	0.4, 3.4 (19%)	1400 (81%)
			B3	
4.0	0.9, 14 (64%)	1200 (36%)	0.3, 2.1 (91%)	1200 (9%)
2.0	0.9, 14 (47%)	1200 (53%)	0.3, 2.1 (90%)	1200 (10%)
1.0	0.9, 14 (28%)	1200 (72%)	0.3, 2.1 (85%)	1200 (15%)
0.5	0.9, 14 (11%)	1200 (89%)	0.3, 2.1 (50%)	1200 (50%)

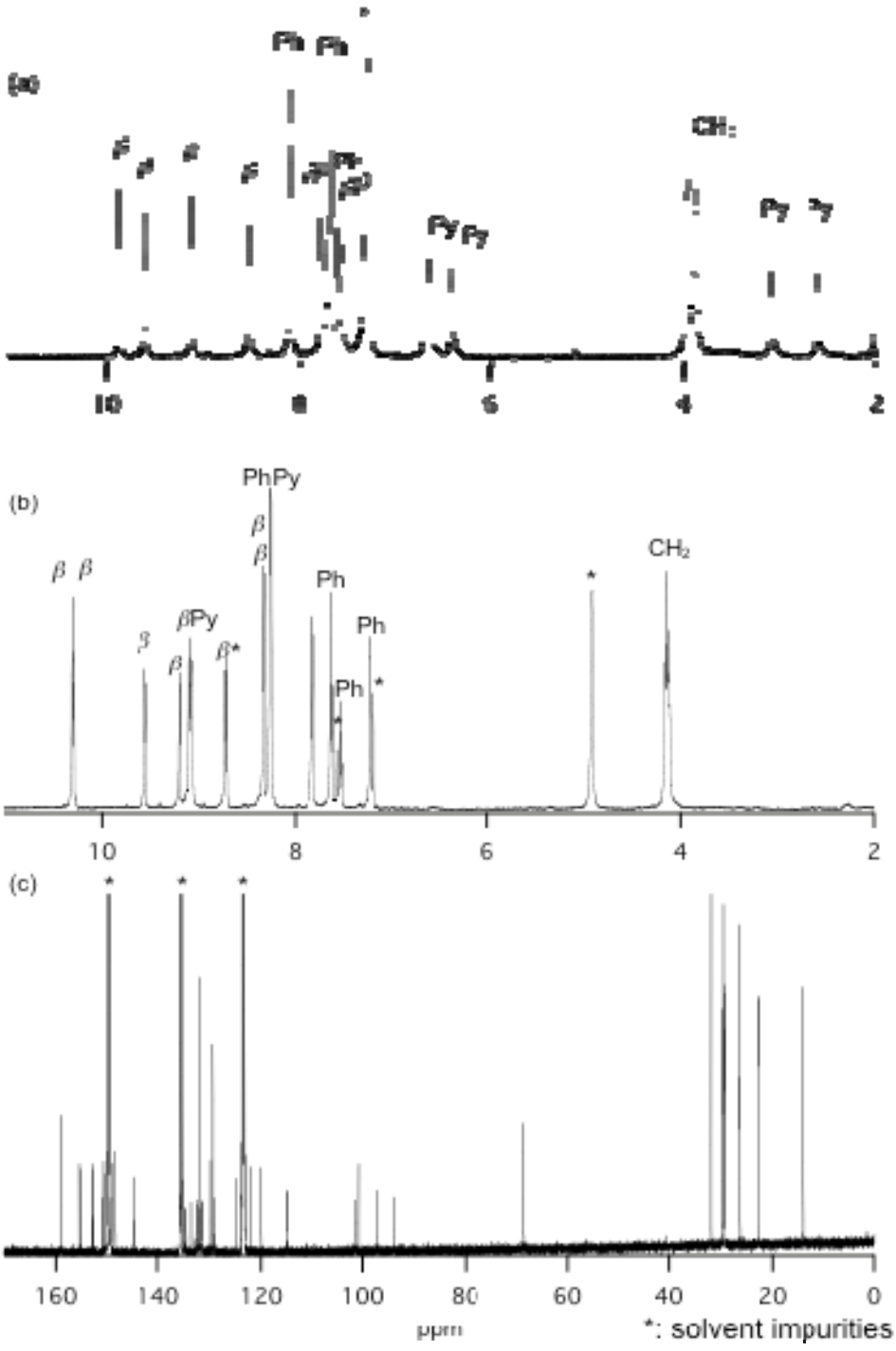

Figure S1. NMR spectra of **D2** (a) ^{1}H in $CDCl_3$, (b) ^{1}H in pyridine-d_5, (c) ^{13}C in pyridine-d_5.

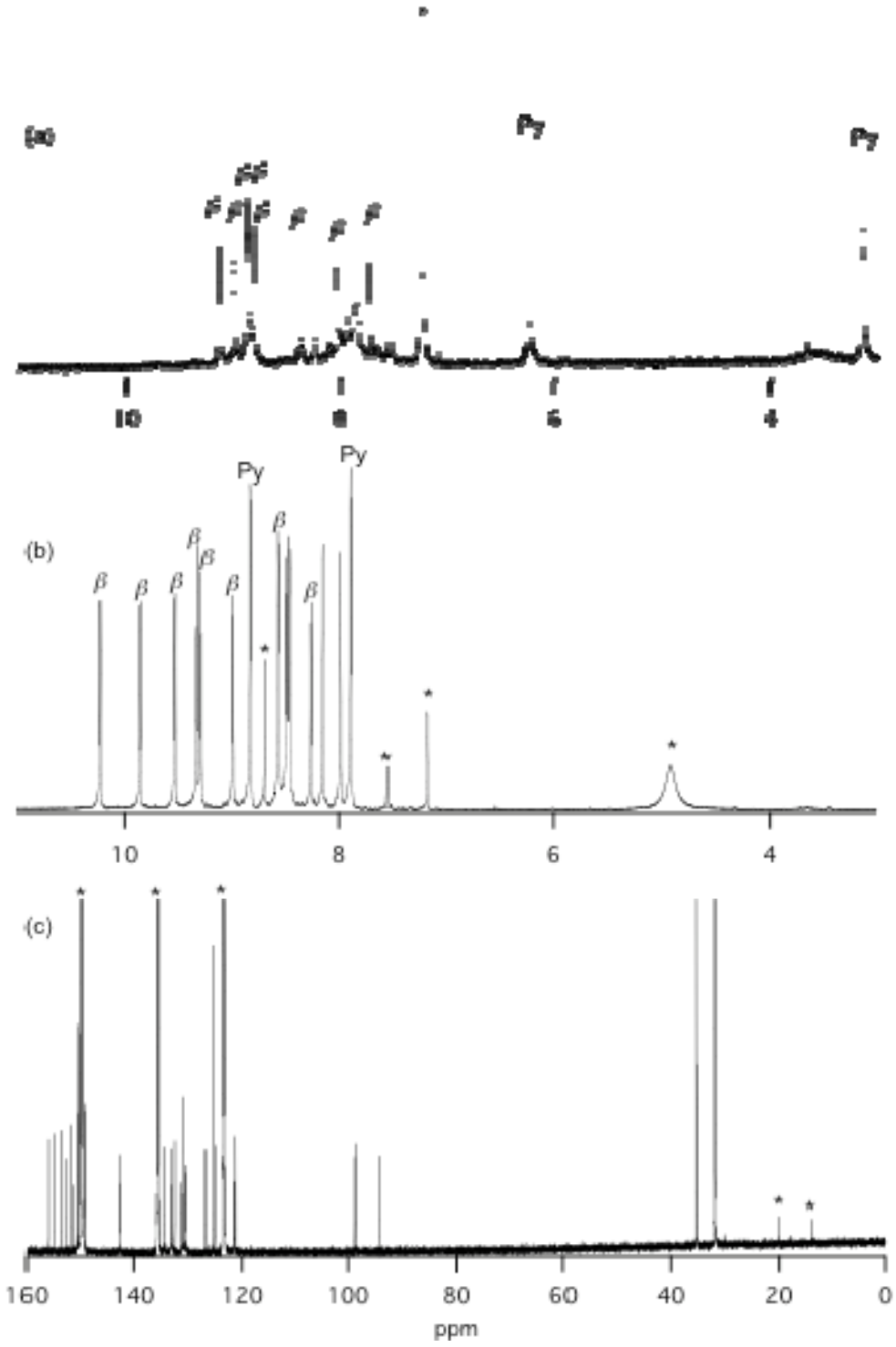

Figure S2. NMR spectra of **D3** (a) ^{1}H in $CDCl_3$, (b) ^{1}H in pyridine-d_5, (c) ^{13}C in pyridine-d_5.

Analytical GPC-HPLC Chromatograms

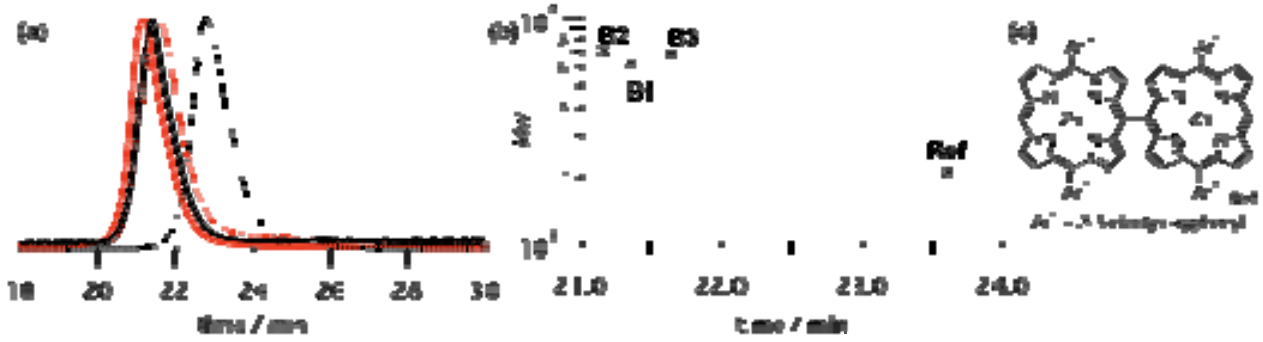

Figure S3. (a) Analytical GPC-HPLC chromatograms (black solid line: **B1**; red solid line: **B2**; red dotted line: **B3**; and black dotted line: reference compound; eluted with $CHCl_3$). (b) Relationship between *Mw* vs retention times. (c) Structure of reference compound.

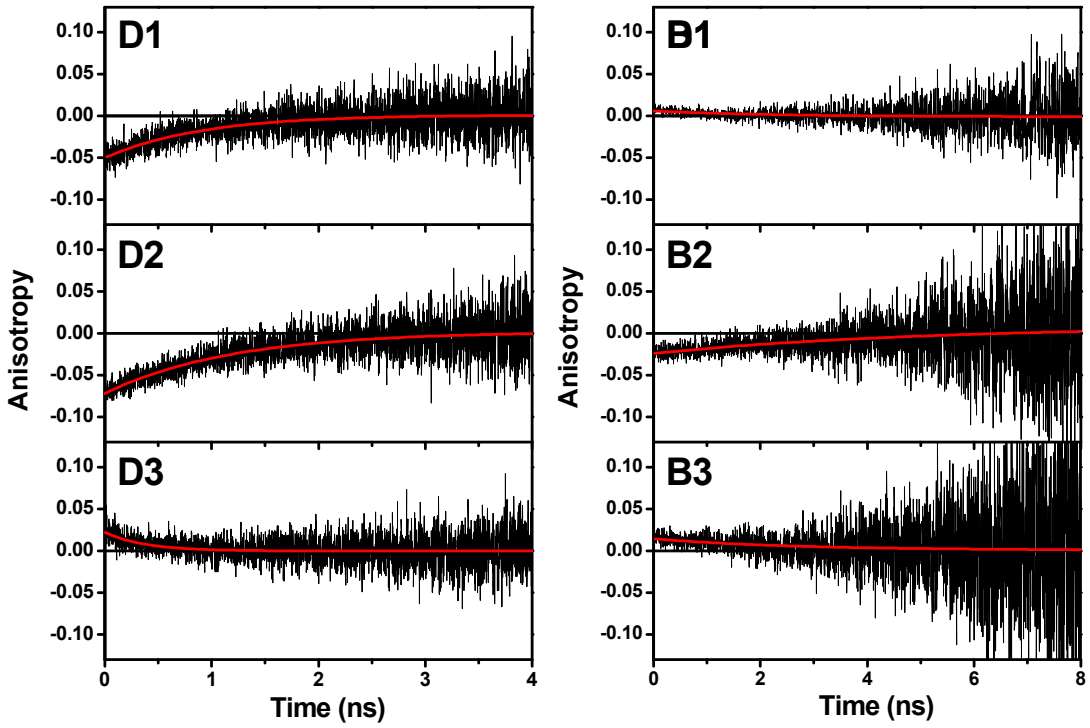

Figure S4. Time-resolved fluorescence anisotropy decay profiles of **D*n*** and **B*n***. The polarized fluorescence decays (I_{VV}(t) and I_{VH}(t)) were measured using the excitation wavelengths of 420 nm (**D1**/**B1**), 450 nm (**D2**/**B2**, **D3**/**B3**) and emission wavelength of 630 nm (**D1**/**B1**), 650 nm (**D2**/**B2**, **D3**/**B3**) and then, the anisotropy decay r(t) was calculated.

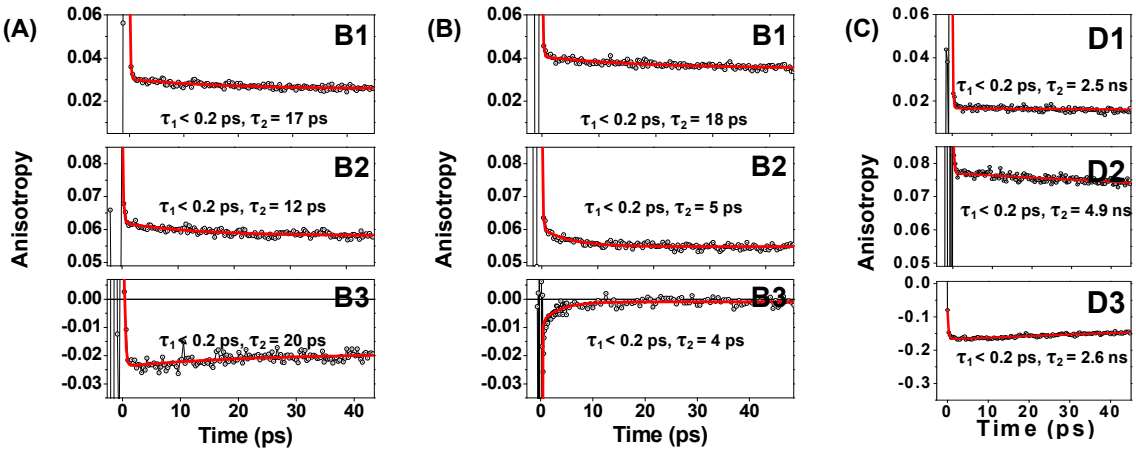

Figure S5. Transient absorption anisotropy decay profiles of **B*n***. The fitted anisotropy decay parameters are listed at the bottom of each panel. The transient absorption anisotropy decay profiles of **D*n*** are shown in the right side. The pump wavelengths were 570 nm and probe wavelength was 520 nm.